Post-print of: J Bacteriol. 2011 December; 193(24): 6815–6823.

FraH Is Required for Reorganization of Intracellular Membranes during Heterocyst Differentiation in Anabaena sp. Strain PCC 7120 [down-pointing small open triangle] †

Victoria Merino-Puerto (1) Vicente Mariscal (1)Heinz Schwarz (2) Iris Maldener (3) Conrad W. Mullineaux (4) Antonia Herrero (1) and Enrique Flores (1)

(1) Instituto de Bioquímica Vegetal y Fotosíntesis, Consejo Superior de Investigaciones Científicas and Universidad de Sevilla, Seville, Spain

(2) Max Planck Institute for Developmental Biology, Spemannstrasse 35, 72076 Tübingen, Germany

(3) IMIT, Microbiology/Organismic Interactions, Department of Biology, University of Tübingen, Auf der Morgenstelle 28, 72076 Tübingen, Germany

(4 School of Biological and Chemical Sciences, Queen Mary University of London, Mile End Road, London E1 4NS, United Kingdom

Abstract

In the filamentous, heterocyst-forming cyanobacteria, two different cell types, the CO2-fixing vegetative cells and the N2-fixing heterocysts, exchange nutrients and regulators for diazotrophic growth. In the model organism Anabaena sp. strain PCC 7120, inactivation of fraH produces filament fragmentation under conditions of combined nitrogen deprivation, releasing numerous isolated heterocysts. Transmission electron microscopy of samples prepared by either high-pressure cryo-fixation or chemical fixation showed that the heterocysts of a ΔfraH mutant lack the intracellular membrane system structured close to the heterocyst poles, known as the honeycomb, that is characteristic of wild-type heterocysts. Using a green fluorescent protein translational fusion to the carboxyl terminus of FraH (FraH-C-GFP), confocal microscopy showed spots of fluorescence located at the periphery of the vegetative cells in filaments grown in the presence of nitrate. After incubation in the absence of combined nitrogen, localization of FraH-C-GFP changed substantially, and the GFP fluorescence was conspicuously located at the cell poles in the heterocysts. Fluorescence microscopy and deconvolution of images showed that GFP fluorescence originated mainly from the region next to the cyanophycin plug present at the heterocyst poles. Intercellular transfer of the fluorescent tracers calcein (622 Da) and 5-carboxyfluorescein (374 Da) was either not impaired or only partially impaired in the ΔfraH mutant, suggesting that FraH is not important for intercellular molecular exchange. Location of FraH close to the honeycomb membrane structure and lack of such structure in the ΔfraH mutant suggest a role of FraH in reorganization of intracellular membranes, which may involve generation of new membranes, during heterocyst differentiation.

INTRODUCTION

Cyanobacteria such as those of the genera Anabaena and Nostoc grow as filaments of cells (trichomes) that, when incubated in the absence of a source of combined nitrogen, present two cell types: vegetative cells that perform oxygenic photosynthesis with concomitant CO2

fixation and heterocysts that perform N2 fixation (11). In Anabaena and Nostoc, heterocysts are spaced along the filament and differentiate from vegetative cells in a process that involves execution of a specific program of gene expression and intercellular transfer of regulators (14, 20, 32, 44). Heterocyst differentiation starts as a response to N deprivation mediated by the global N-control transcription factor of cyanobacteria, NtcA (14), and requires the early-acting differentiation-specific factor HetR (3, 4). In the N2-fixing filament, heterocysts provide the vegetative cells with fixed nitrogen, and the vegetative cells provide heterocysts with photosynthate (43). Thus, both regulators and nutrients are likely exchanged between cells in the cyanobacterial filaments.

The cyanobacteria are diderm bacteria (37) carrying an outer membrane (OM) outside the cytoplasmic membrane (CM) and the peptidoglycan layer (11, 20). In filamentous cyanobacteria, whereas the CM and peptidoglycan layer surround each cell, the OM is continuous along the filament (12, 23, 33, 41). Differentiation of a vegetative cell into a heterocyst involves several morphological changes, including the deposition of an extra cell envelope and the reorganization of intracellular membranes (21, 43). The heterocyst envelope includes an outer polysaccharide layer and an inner glycolipid layer that are deposited outside the OM (12, 21). The thylakoids (photosynthetic membranes), which are largely located in the periphery of vegetative cells, are subjected during heterocyst differentiation to a strong reorganization that may also involve generation of new membranes, producing a largely packaged membrane structure known as “honeycomb” (21). Additionally, some peripheral intracellular membranes remain in the heterocyst. The honeycomb is located close to the heterocyst poles, next to the cyanophycin plug that is associated with the heterocyst “neck” (21, 35). Cyanophycin is multi-l-arginyl-poly-(l-aspartic acid), a nitrogen reserve that accumulates after nitrogenase activity peaks late in differentiation (35). Location of the honeycomb correlates with the place of oxidation of diaminobenzidine in heterocysts in the dark, which is indicative of respiratory activity (28, 43). Thus, the reorganization of intracellular membranes can reflect adaptation to the specialized bioenergetics of the heterocyst, which depends on photosystem I activity and dedicated terminal respiratory oxidases (17, 38, 39, 43).

In the model heterocyst-forming cyanobacterium Anabaena sp. strain PCC 7120, genes whose mutation results in filament fragmentation, some of which could encode cell-cell joining proteins, are known (2, 5, 9, 13, 25, 29). The genes in the fraCDE operon are required for Anabaena to make long filaments mainly under N2-fixing conditions (25). The sepJ gene (also known as fraG [29]) is required for filament integrity in the presence or absence of combined N (13). Using fusions to the green fluorescent protein (GFP), we have previously shown that FraC, FraD, and SepJ are located in the intercellular septa of the Anabaena filaments, in which SepJ is particularly focused at the cell poles, and that SepJ localization is altered in fraC and fraD mutants (13, 22, 25). Intercellular molecular exchange in Anabaena spp. can be probed with fluorescent tracers such as calcein or 5-carboxyfluorescein (5-CFDA) (24, 27). Calcein transfer is impaired in sepJ, fraC, and fraD mutants, pointing to an important role of at least SepJ in intercellular molecular exchange (25, 27). These studies have led to the notion that these proteins may constitute cell-cell joining complexes that bind the cells and facilitate intercellular molecular exchange in the cyanobacterial filament (24–27).

The fraH gene (open reading frame [ORF] alr1603 of the Anabaena sp. strain PCC 7120 genomic sequence [19]) is also required for filament integrity under diazotrophic conditions (2, 25). The fraH mutants are impaired in diazotrophic growth but form heterocysts that exhibit negligible nitrogenase activity. In contrast to fraC or fraD mutants, a ΔfraH mutant is not impaired in localization of SepJ and can transfer calcein between vegetative cells, albeit at

lower rates than the wild type (25). Here, we addressed the subcellular localization of FraH and the effect of its inactivation on the ultrastructure of the Anabaena cells, and we provide a detailed analysis of intercellular transfer of fluorescent tracers in the ΔfraH mutant compared to that in the wild type. Our results suggest a role of FraH in reorganization or generation of intracellular membranes during heterocyst differentiation.

MATERIALS AND METHODS

Strains and growth conditions.

Anabaena sp. strain PCC 7120 (also known as Nostoc sp. strain PCC 7120) and strain CSVT4, which carries an unmarked deletion of the fraH gene (25), were grown in BG11 medium (containing ferric citrate instead of ferric ammonium citrate [31] and $NaNO_3$ as the nitrogen source) or BG110 medium (free of combined nitrogen) at 30°C in light (about 25 μE m^{-2} s^{-1}) in shaken (90 to 100 rpm) liquid cultures or in medium solidified with 1% Difco agar. Alternatively, cultures (referred to as bubbled cultures and denoted BG11C or BG110C) were supplemented with 10 mM $NaHCO_3$ and bubbled with a mixture of air and 1% (vol/vol) CO_2 in light (75 μE m^{-2} s^{-1}).

Genetic procedures.

DNA was isolated from Anabaena sp. by the method of Cai and Wolk (6). PCR was performed by standard procedures (1), and the PCR products were resolved by electrophoresis in 0.7% agarose gels.

To prepare an Anabaena strain producing a fusion of the GFP to FraH, a DNA fragment comprising the sequence from nucleotide −124 to nucleotide +867 relative to the start of the fraH gene was amplified by PCR. PCR was performed using genomic DNA of strain PCC 7120 as a template and primers fraH-1 (5′-GCC TTG CTG CAT TTC TCA) and fraH-16 (5′-CCC GGG AGC GAG TTT AAA GAG GA), the latter including an SmaI restriction site. The 997-bp PCR product was cloned in pGEM-T, confirmed by sequencing, and transferred as a SacI-SmaI fragment to SacI-EcoRV-digested pCSAM135 (13), producing a fusion of the fraH coding sequence (stop codon removed) to the gfp-mut2 gene. This construct was transferred as a KpnI restriction fragment to pCSV3 (40), producing pCSVT70, in which the fraH-gfp fusion was confirmed by sequencing. pCSVT70 was then transferred by conjugation from Escherichia coli to Anabaena sp. strain PCC 7120 as described previously (8). Clones resistant to streptomycin (5 μg ml^{-1}) and spectinomycin (5 μg ml^{-1}) were isolated, and integration of the fraH-gfp construct was verified by PCR using primers F9 and gfp-4 (25).

Electron microscopy.

For transmission electron microscopy (TEM) two different methods were performed using high-pressure cryo-fixation and chemical fixation. For high-pressure cryo-fixation, filaments grown in BG11 medium or incubated in BG110 medium for 48 h in the light on a shaker were harvested and infiltrated into cellulose capillary tubes (15), transferred to 150-μm-deep aluminum planchettes filled with hexadecane, and frozen under high pressure in a Bal-Tec HPM 010 freezing device. The samples were freeze-substituted in a Leica AFS2 unit (starting at −90°C up to −40°C) in 0.5% uranyl acetate in acetone, infiltrated at −40°C with Epon resin, and UV polymerized. To visualize morphology by chemical fixation, the filaments were fixed with 2.5% glutaraldehyde and 2% $KMnO_4$, dehydrated with increasing concentrations of ethanol, and embedded in Epon, and ultra-thin sections were prepared and poststained with 1% uranyl

acetate and lead citrate (10). The samples were examined with a Philips CM10 electron microscope at 60 kV.

Confocal and fluorescence microscopy.

Small blocks of agar-solidified medium (BG11 or BG110) carrying the filaments were cut and placed in a sample holder with a glass coverslip on top. For confocal microscopy of GFP fluorescence, filaments of cells were visualized using a Leica HCX Plan-APO 63× oil immersion objective (numerical aperture, 1.4) attached to a Leica TCS SP2 confocal laser scanning microscope. GFP was excited using 488-nm irradiation from an argon ion laser. Fluorescent emission was monitored by collection across windows of 500 to 540 nm (GFP imaging) and 630 to 700 nm (cyanobacterial autofluorescence).

For fluorescence microscopy, filaments of cells were imaged using a Leica DM6000B fluorescence microscope and an ORCA-ER camera (Hamamatsu). GFP fluorescence was monitored using a fluorescein isothiocyanate (FITC) L5 filter (excitation, band-pass [BP] 480/40 filter; emission, BP 527/30 filter), and red autofluorescence was monitored using a Texas Red TX2 filter (excitation, BP 560/40; emission, BP 645/75). Images were convolved with the Leica Application Suite Advanced Fluorescence software.

Calcein and 5-carboxyfluorescein labeling and fluorescence recovery after photobleaching (FRAP).

For labeling with fluorescent tracers, 1 ml of cell cultures was harvested, washed, resuspended in 1 ml of fresh growth medium, and then mixed with 4 µl of 5-carboxyfluorescein diacetate acetoxymethyl ester ([AM] 5 mg/ml in dimethyl sulfoxide) or 20 µl of calcein AM (1 mg/ml dimethyl sulfoxide). The suspension was incubated in dim light at 30°C for 30 min, and filaments were then harvested and washed three times in fresh, dye-free growth medium. Filament suspensions were spotted onto agar with BG11 or BG110 medium and placed in a custom-built temperature-controlled sample holder with a glass coverslip on top. All measurements were carried out at 30°C.

For both calcein and 5-CFDA FRAP, the cells were visualized by confocal microscopy as above, using a 488-nm-line argon laser as the excitation source. Fluorescence emission was monitored by collection across windows of 500 to 520 nm or 500 to 527 nm in different experiments and a 100-µm pinhole. After an initial image was recorded, the bleaching was carried out by switching the microscope to x-scanning mode, increasing the laser intensity by a factor of 10, and scanning a line across one cell for 0.137 s. The laser intensity was then reduced, the microscope was switched back to xy-imaging mode, and a sequence of images was recorded typically at 2-s intervals for 20 s.

FRAP data analysis was made using ImageJ, version 1.41, software (http://rsbweb.nih.gov/ij/). Determination of the exchange coefficient, E, in the transfer of calcein between vegetative cells and heterocysts was performed as described previously (27). For 5-carboxyfluorescein, we observed that there was an immobile fraction of about 50% of 5-carboxyfluorescein in nonbleached cells, which was inadequate for use in the equations to determine E. We observed, however, that recovery of 5-carboxyfluorescein fluorescence in bleached cells best fit an exponential curve: $CB = C0 + CR(1 - e^{-2Rt})$ for intercalary cells or $CB = C0 + CR(1 - e^{-Rt})$ for cells terminally located in the filament, where CB is fluorescence in the bleached cell, C0 is fluorescence immediately after the bleach and tending toward (C0 + CR) after fluorescence recovery, R is the recovery rate constant, and t is time. These formulae were used to calculate

R, which represents the recovery rate constant due to transfer of 5-carboxyfluorescein from one neighbor cell.

Bioinformatic protein sequence analysis.

Protein topology predictions were performed using a variety of programs included in the ExPASy Proteomic Service (http://www.expasy.ch/tools/) and the PSIPRED Protein Structure Prediction Server (http://bioinf.cs.ucl.ac.uk/psipred/). Protein sequences were retrieved from the Kazusa DNA Research Institute (http://genome.kazusa.or.jp/cyanobase/) and the Department of Energy (DOE) Joint Genome Institute (http://img.jgi.doe.gov/).

RESULTS

Electron microscopy of a ΔfraH mutant.

A mutant of Anabaena sp. strain PCC 7120 carrying an in-frame deletion of fraH, strain CSVT4, has been previously isolated (25). Nitrate-grown filaments of strain CSVT4 hardly showed any alteration, compared to the wild type, that could be observed by TEM (data not shown). In contrast, filaments incubated for 48 h in the absence of combined nitrogen contained aberrant heterocysts. Figure 1a and b show heterocysts of the wild-type strain, PCC 7120, and of strain CSVT4 as observed by TEM after high-pressure cryo-fixation (see Materials and Methods). The wild-type heterocyst shows the heterocyst-specific polysaccharide and glycolipid layers (the latter can be better appreciated after chemical fixation) (see Fig. 2c), the cyanophycin plugs at its poles, and the characteristic arrangements of intracellular membranes that are concentrated next to the cyanophycin plugs (the so-called honeycomb structures). These features are well-known characteristics of heterocysts (43). Some of these heterocyst morphological features can be observed in the heterocysts of mutant strain CSVT4. The heterocyst in Fig. 1b bears the polysaccharide and glycolipid layers, which is consistent with the previous finding of heterocyst glycolipids and cells positively staining with Alcian blue in filaments of strain CSVT4 (25), and a clear cyanophycin plug in its pole close to a vegetative cell. (A terminal heterocyst, such as that shown in Fig. 1b, has the characteristic heterocyst neck only in its pole proximal to an adjacent vegetative cell.) On the other hand, the CSVT4 heterocyst showed peripheral intracellular membranes but not the honeycomb structure of intracellular membranes arranged around the heterocyst pole (Fig. 1b). After chemical fixation, wild-type heterocysts observed by TEM also showed the characteristic heterocyst features (Fig. 1c), whereas CSVT4 heterocysts were again observed to lack the honeycomb structure (two examples are shown in Fig. 1d). Lack of the honeycomb structure constitutes a characteristic of mutant CSVT4 since we did not observe this structure in any of a total of 24 different CSVT4 heterocysts observed by TEM after either cryo- or chemical fixation.

Some doublets of cells encapsulated in a thickened envelope, likely made of polysaccharide, were observed by TEM in the preparation of CSVT4 filaments (Fig. 2, gray arrows). These structures are likely the result of the division of a cell that has started, but not completed, heterocyst differentiation. Indeed, in the micrograph shown in Fig. 2, an encapsulated cell in the process of division can also be observed (white arrow). An isolated heterocyst, which lacks the honeycomb structure but contains the cyanophycin plug, can also be observed in this micrograph (black arrow).

Subcellular localization of FraH.

FraH is a 289-amino-acid residue acidic protein (pKi, 4.40) of uncertain topology although some prediction programs suggest the presence of one transmembrane segment (amino acid

residues 241 to 260) (Fig. 3A, gray region), with the C terminus located in the cytoplasm and a substantial part of the protein in the periplasm. Other remarkable sequence features include an N-terminal segment (amino acid residues 4 to 48) (Fig. 3A, red region) with four regularly spaced Cys-X-X-Cys motifs, a proline-rich region (amino acid residues 58 to 215; 27.8% proline) (Fig. 3A, blue region), and a forkhead-associated domain (FHA; amino acid residues 204 to 260) (Fig. 3A, approximate location is shown). FHA domains are involved in interaction with phospho-peptides and mediate signal transduction in Ser/Thr kinase signaling networks in bacteria as well as in eukaryotes (30).

To investigate the localization of FraH in the Anabaena filaments, strain CSVT26, which produces a fusion protein in which the GFP is added to the last (C-terminal) amino acid residue of FraH (FraH-C-GFP), was constructed. This strain was generated by single recombination of a fraH-gfp-mut2 fusion gene (cloned in a plasmid) with the resident fraH gene so that the whole fraH-gfp-mut2-carrying plasmid was integrated into the chromosome, producing a duplication of fraH sequences, including a wild-type fraH gene. Strain CSVT26 grow diazotrophically.

In nitrate-grown filaments of strain CSVT26, the GFP fluorescence was observed by confocal microscopy as spots that appeared to reside in the periphery of the cells, and in some filaments the spots could be seen in a helical pattern (Fig. 3B). Analysis by fluorescence microscopy permitted further observations of the peripheral localization of FraH-C-GFP, which appeared to reside outside the chlorophyll a-containing membranes, which are identified by their red autofluorescence (Fig. 3C). The peripheral location of FraH-C-GFP could be further visualized by rotation of the strain CSVT26 filaments (see Movie S1 in the supplemental material).

After incubation for 24 h in the absence of combined nitrogen, the FraH-C-GFP signals were evident in the heterocysts, where they localized to the cell poles (Fig. 3D). A small fluorescent spot was also frequently observed in the proximal cell pole of a vegetative cell next to a heterocyst. Thus, in Fig. 3D, arrows 1 and 2 indicate an intercalary and a terminal heterocyst, respectively, in whose adjacent vegetative cells a small GFP spot can be observed. In contrast, no such spots are observed in the vicinity of an isolated proheterocyst (arrow 3), confirming that the small spot resides in the adjacent cell. (The cell marked by arrow 3 is denoted a proheterocyst because it shows substantial red autofluorescence, which largely disappears from mature heterocysts.) Although not observed in this micrograph, vegetative cells of diazotrophic filaments also showed some FraH-C-GFP fluorescence spots (see below).

To ascertain the time point in heterocyst differentiation at which the FraH-C-GFP protein localized to the cell poles, time course experiments were performed (Fig. 4). The GFP spots in the vegetative cells became hardly visible after 9 h of nitrogen deprivation, becoming more evident again and mostly localized to the poles of cells that were discernible as proheterocysts or heterocysts at 14 and 24 h of nitrogen deficiency, respectively. GFP spots were still observed, however, in the vegetative cells of the diazotrophic filament. Identical results were found with two different clones of strain CSVT26 (Fig. 4 and data not shown).

Intercellular transfer of calcein and 5-carboxyfluorescein.

We have previously shown that, unlike in a sepJ mutant and the ΔfraC and ΔfraD mutants, intercellular transfer of the 622-Da tracer calcein is only partly impaired in strain CSVT4 (25, 27). Transfer of a smaller tracer, 5-carboxyfluorescein (374 Da), is, however, only partly impaired in the ΔsepJ mutant, strain CSVM34 (24), but largely hampered in ΔfraC and ΔfraD mutants (26). We therefore investigated transfer of 5-carboxyfluorescein in the ΔfraH mutant

using the wild type as a control. Transfer between vegetative cells in filaments grown with nitrate as the nitrogen source or incubated in the absence of combined nitrogen for 24 h was tested by means of FRAP experiments. Figure 6A shows examples of 5-carboxyfluorescein FRAP with filaments of the wild type and strain CSVT4, both of which showed substantial transfer. Figure 6B summarizes the results obtained with the two investigated strains quantified and presented as the recovery rate constant, R (see Materials and Methods for details). Whereas in nitrate-grown filaments, transfer in the mutant was similar to that observed for the wild type, in filaments incubated without combined nitrogen for 24 h, transfer was about 73% of the level observed in the wild type.

Because of the polar location of FraH in the heterocysts, we were interested in testing transfer of the tracer between vegetative cells and heterocysts. Unfortunately, because of poor labeling of the heterocysts, we could not determine 5-carboxyfluorescein transfer between vegetative cells and heterocysts. In contrast, calcein labels heterocysts as well as vegetative cells (27). We therefore performed FRAP experiments bleaching the calcein and following fluorescence recovery in heterocysts. Results similar to those previously reported (24, 25, 27) were obtained for the wild type after both 24 and 48 h of nitrogen deprivation (Fig. 7). For mutant strain CSVT4, the analysis had to be restricted, of course, to heterocysts that remained bound to vegetative cells (normally terminal heterocysts in short filaments). For this strain, exchange coefficient (E) values (see Materials and Methods) were double those of the wild type (Fig. 7B). On the other hand, as expected, no recovery of fluorescence was observed after the photobleaching of an isolated heterocyst (Fig. 7A, bottom).

DISCUSSION

We have investigated FraH cellular and subcellular localization using a fusion of the GFP to its carboxyl terminus (FraH-C-GFP). Fluorescence from FraH-C-GFP was readily detected, and because the GFP is expected to fold properly only in the cytoplasm (7), the observed fluorescence pattern is consistent either with the protein being cytoplasmic or with anchoring of the protein to the CM, with its carboxyl end located in the cytoplasm. In vegetative cells, FraH-C-GFP appears to reside in the periphery of the cells outside the chlorophyll a-containing membranes (Fig. 3C). Whether FraH is inserted into the CM through a transmembrane segment or is peripherally bound to the CM or, alternatively, is somehow associated with the most external surface of the thylakoid remains to be established.

Although FraH-C-GFP can be observed in the vegetative cells of nitrate-grown and diazotrophic filaments, in diazotrophic filaments it is conspicuously located at the heterocyst poles (Fig. 3D). The presence of FraH-C-GFP in cultures in the presence and absence of combined nitrogen is consistent with previous observations of a substantial expression of fraH in ammonium-containing cultures and a further increase in transcript levels under nitrogen deprivation (25). This increase is impaired in ntcA and hetR mutants, which would be consistent with induction taking place largely in the cells that are differentiating into heterocysts. In a proteomic analysis of filaments grown with or without combined nitrogen, FraH was also found at 2-fold higher levels in the diazotrophic cultures (36). As observed in this work (Fig. 4), the FraH-C-GFP fluorescence changes substantially during adaptation to nitrogen deficiency, resulting in a preferential localization of FraH-C-GFP at the heterocyst poles in the diazotrophic filament. Relocalization of a protein during heterocyst differentiation represents a novel aspect of development in these organisms.

The helical arrangement of FraH-C-GFP observed in some cells (Fig. 3B) is reminiscent of the subcellular localization of some bacterial cytoskeletal proteins such as MreB that makes a

helical filament underneath the CM (18). The Anabaena homologue of MreB has been inactivated, showing that this protein is needed to maintain the normal morphology of this cyanobacterium, whose cells tend to be cylindrical in shape, but the authors failed to show a helical pattern of the MreB protein itself (16). Further work will be necessary to test a relationship of FraH to the cytoskeleton, including a possible role of the latter in relocalization of FraH to the cell poles during heterocyst differentiation. In this context, the known role of MreB directing polar localization of a number of different proteins in several bacteria is of interest (reviewed in reference 34).

Using transmission electron microscopy of samples subjected to cryo-fixation or chemical fixation, we have observed that heterocysts produced in the ΔfraH mutant, strain CSVT4, strikingly lack the honeycomb structure. This is suggestive of a defect in intracellular membrane reorganization, which may involve generation of new membranes, during heterocyst differentiation. Alternatively, the honeycomb structure could not be formed in strain CSVT4 because of an early arrest in heterocyst differentiation or as a consequence, somehow, of filament fragmentation. However, because the cyanophycin plug is observed in CSVT4 heterocysts that lack the honeycomb structure (Fig. 1) and a honeycomb structure is present in other filament fragmentation mutants, such as the ΔfraC or ΔfraD mutant (26), these possibilities are unlikely. Nonetheless, the presence in CSVT4 filament suspensions of some cells that, after having apparently started differentiation, have completed cell division, resulting in cell doublets encapsulated in what appears to be a polysaccharide envelope, suggests that deletion of fraH has also a leaky early differentiation defect. We define this phenotype as leaky because it is not always expressed, and cultures of CSVT4 incubated in the absence of combined nitrogen contain many distinguishable heterocysts that are defective as discussed above. We have previously observed this phenomenon (division within a thickened cell envelope) in a sepJ mutant, which aborts differentiation very early in the process (13), and a similar structure has also been observed for a fraC mutant (2).

A defect in intracellular membrane reorganization during heterocyst differentiation in the ΔfraH mutant is consistent with the observed localization of FraH-C-GFP close to the cyanophycin plugs in the heterocysts (Fig. 5), where the honeycomb structure also resides. The honeycomb structure is likely essential for the bioenergetics of the heterocysts as well as for reduction of traces of oxygen, and lack of such structure is consistent with lack of nitrogenase activity in heterocyst-containing CSVT4 filaments, which nonetheless express at normal levels the nifHDK genes, encoding nitrogenase (25). A defect in production of the honeycomb membrane structure has also been previously noticed in a mutant, strain CSAV141, of the two terminal respiratory oxidases that are specifically expressed in the heterocysts of Anabaena sp. strain PCC 7120 (39). However, under anoxic conditions, strain CSAV141 shows significant nitrogenase activity (39) that is not observed in strain CSVT4 (25). The intracellular membranes in the heterocysts of strain CSAV141 may not mature because they lack bioenergetic complexes normally located in them, and, in a similar way, those membranes may not form in strain CSVT4 because of a role of FraH in them. However, FraH could also have a direct role in membrane reorganization, including the development of the honeycomb structure, during heterocyst differentiation. The possible existence of proteins required for generation of honeycomb membranes has been previously considered (42).

The fraH gene is located downstream of a gene encoding 6-phosphogluconolactonase, an enzyme of the pentose-phosphate pathway, in all available genomes of heterocyst-forming cyanobacteria as well as in those of many other cyanobacteria. In Anabaena sp. strain PCC 7120, both genes, alr1602 and alr1603 (fraH), can be expressed as independent transcripts as

well as in a common transcript (25). Inactivation of alr1602 results in the inability to grow diazotrophically (44). These observations suggest a concerted action of the products of both genes. Although a possible mechanism remains to be investigated, we note the importance of the oxidative pentose-phosphate pathway in heterocysts (11, 44).

The fraH gene was initially described as a gene whose mutation produces filament fragmentation with a noticeable release of free heterocysts in medium lacking combined nitrogen (2). Further characterization corroborated the filament fragmentation phenotype and a defect in diazotrophic growth of a fraH deletion mutant (25), but how filament fragmentation relates to production of an immature heterocyst in fraH mutants is unknown. Proteins SepJ, FraC, and FraD, which are required for filament integrity, are also required for normal intercellular transfer of fluorescent tracers in Anabaena sp. strain PCC 7120. Inactivation of sepJ impairs intercellular transfer of calcein more than transfer of 5-carboxyfluorescein (24), whereas inactivation of fraC or fraD substantially hampers transfer of both tracers (25, 26). In the fraH mutants, however, transfer between vegetative cells of both calcein and 5-carboxyfluorescein was either not affected or only partially affected (reference 25 and this work). Therefore, in contrast to other proteins required for filament integrity, FraH appears not to be needed for intercellular molecular exchange, which is consistent with a different role for FraH, as discussed above. On the other hand, transfer of calcein from vegetative cells to heterocysts was increased in strain CSVT4 compared to the wild-type strain (Fig. 7). It is possible that the honeycomb membranes reduce the rate of calcein influx into heterocysts, as we have previously observed for the cyanophycin plugs (27).

ACKNOWLEDGMENTS

We thank Brigitte Sailer (MPI, Tübingen, Germany) and Alicia Orea (IBVF, Seville, Spain) for excellent technical assistance.

This work was supported by grant number BFU2008-03811 from the Ministerio de Ciencia y Tecnología (Madrid, Spain), cofinanced by FEDER.

REFERENCES

1. Ausubel F. M., et al. 2011. Current protocols in molecular biology. Wiley-Interscience, New York, NY.

2. Bauer C. C., Buikema W. J., Black K., Haselkorn R. 1995. A short-filament mutant of Anabaena sp. strain PCC 7120 that fragments in nitrogen-deficient medium. J. Bacteriol. 177:1520–1526.

3. Black T. A., Cai Y., Wolk C. P. 1993. Spatial expression and autoregulation of hetR, a gene involved in the control of heterocyst development in Anabaena. Mol. Microbiol. 9:77–84.

4. Buikema W. J., Haselkorn R. 1991. Characterization of a gene controlling heterocyst differentiation in the cyanobacterium Anabaena 7120. Genes Dev. 5:321–330.

5. Buikema W. J., Haselkorn R. 1991. Isolation and complementation of nitrogen fixation mutants of the cyanobacterium Anabaena sp. strain PCC 7120. J. Bacteriol. 173:1879–1885.

6. Cai Y. P., Wolk C. P. 1990. Use of a conditionally lethal gene in Anabaena sp. strain PCC 7120 to select for double recombinants and to entrap insertion sequences. J. Bacteriol. 172:3138–3145.

7. Drew D., et al. 2002. Rapid topology mapping of Escherichia coli inner-membrane proteins by prediction and PhoA/GFP fusion analysis. Proc. Natl. Acad. Sci. U. S. A. 99:2690–2695.

8. Elhai J., Vepritskiy A., Muro-Pastor A. M., Flores E., Wolk C. P. 1997. Reduction of conjugal transfer efficiency by three restriction activities of Anabaena sp. strain PCC 7120. J. Bacteriol. 179:1998–2005.

9. Ernst A., et al. 1992. Synthesis of nitrogenase in mutants of the cyanobacterium Anabaena sp. strain PCC 7120 affected in heterocyst development or metabolism. J. Bacteriol. 174:6025–6032.

10. Fiedler G., Arnold M., Hannus S. I., Maldener 1998. The DevBCA exporter is essential for envelope formation in heterocysts of the cyanobacterium Anabaena sp. strain PCC 7120. Mol. Microbiol. 27:1193–1202.

11. Flores E., Herrero A. 2010. Compartmentalized function through cell differentiation in filamentous cyanobacteria. Nat. Rev. Microbiol. 8:39–50.

12. Flores E., Herrero A., Wolk C. P., Maldener I. 2006. Is the periplasm continuous in filamentous multicellular cyanobacteria? Trends Microbiol. 14:439–443.

13. Flores E., et al. 2007. Septum-localized protein required for filament integrity and diazotrophy in the heterocyst-forming cyanobacterium Anabaena sp. strain PCC 7120. J. Bacteriol. 189:3884–3890.

14. Herrero A., Muro-Pastor A. M., Valladares A., Flores E. 2004. Cellular differentiation and the NtcA transcription factor in filamentous cyanobacteria. FEMS Microbiol. Rev. 28:469–487.

15. Hohenberg H., Mannweiler K., Müller M. 1994. High-pressure freezing of cell suspensions in cellulose capillary tubes. J. Microsc. 175:34–43.

16. Hu B., Yang G., Zhao W., Zhang Y., Zhao J. 2007. MreB is important for cell shape but not for chromosome segregation of the filamentous cyanobacterium Anabaena sp. PCC 7120. Mol. Microbiol. 63:1640–1652.

17. Jones K. M., Haselkorn R. 2002. Newly identified cytochrome c oxidase operon in the nitrogen-fixing cyanobacterium Anabaena sp. strain PCC 7120 specifically induced in heterocysts. J. Bacteriol. 184:2491–2499.

18. Jones L. J. F., Carballido-López R., Errington J. 2001. Control of cell shape in bacteria: helical, actin-like filaments in Bacillus subtilis. Cell 104:913–922.

19. Kaneko T., et al. 2001. Complete genomic sequence of the filamentous nitrogen-fixing cyanobacterium Anabaena sp. strain PCC 7120. DNA Res. 8:205–213.

20. Kumar K., Mella-Herrera R. A., Golden J. W. 2010. Cyanobacterial heterocysts. Cold Spring Harb. Perspect. Biol. 2:a000315.

21. Lang N. J., Fay P. 1971. The heterocysts of blue-green algae. II. Details of ultrastructure. Proc. R. Soc. Lond. B Biol. Sci. 178:193–203.

22. Mariscal V., Flores E. 2010. Multicellularity in a heterocyst-forming cyanobacterium: pathways for intercellular communication. Adv. Exp. Med. Biol. 675:123–135.

23. Mariscal V., Herrero A., Flores E. 2007. Continuous periplasm in a filamentous, heterocyst-forming cyanobacterium. Mol. Microbiol. 65:1139–1145.

24. Mariscal V., Herrero A., Nenninger A., Mullineaux C. W., Flores E. 2011. Functional dissection of the three-domain SepJ protein joining the cells in cyanobacterial trichomes. Mol. Microbiol. 79:1077–1088.

25. Merino-Puerto V., Mariscal V., Mullineaux C. W., Herrero A., Flores E. 2010. Fra proteins influencing filament integrity, diazotrophy and localization of septal protein SepJ in the heterocyst-forming cyanobacterium Anabaena sp. Mol. Microbiol. 75:1159–1170.

26. Merino-Puerto V., et al. 2011. FraC/FraD-dependent intercellular molecular exchange in the filaments of a heterocyst-forming cyanobacterium, Anabaena sp. Mol. Microbiol. 82:87–98.

27. Mullineaux C. W., et al. 2008. Mechanism of intercellular molecular exchange in heterocyst-forming cyanobacteria. EMBO J. 27:1299–1308.

28. Murry M. A., Olafsen A. G., Benemann J. R. 1981. Oxidation of diaminobenzidine in the heterocysts of Anabaena cylindrica. Curr. Microbiol. 6:201–206.

29. Nayar A. S., Yamaura H., Rajagopalan R., Risser D. D., Callahan S. M. 2007. FraG is necessary for filament integrity and heterocyst maturation in the cyanobacterium Anabaena sp. strain PCC 7120. Microbiology 153:601–603.

30. Pennell S., et al. 2010. Structural and functional analysis of phosphothreonine-dependent FHA domain interactions. Structure 18:1587–1595.

31. Rippka R., Deruelles J., Waterbury J. B., Herdman M., Stanier R. Y. 1979. Generic assignments, strain histories and properties of pure cultures of cyanobacteria. Microbiology 111:1–61.

32. Risser D. D., Callahan S. M. 2009. Genetic and cytological evidence that heterocyst patterning is regulated by inhibitor gradients that promote activator decay. Proc. Natl. Acad. Sci. U. S. A. 106:19884–19888.

33. Schneider D., Fuhrmann E., Scholz I., Hess W. R., Graumann P. L. 2007. Fluorescence staining of live cyanobacterial cells suggest non-stringent chromosome segregation and absence of a connection between cytoplasmic and thylakoid membranes. BMC Cell Biol. 8:39.

34. Shaevitz J. W., Gitai Z. 2010. The structure and function of bacterial actin homologs. Cold Spring Harb. Perspect. Biol. 2:a000364.

35. Sherman D. M., Tucker D., Sherman L. A. 2000. Heterocyst development and localization of cyanophycin in N2-fixing cultures of Anabaena sp. PCC 7120 (cyanobacteria). J. Phycol. 36:932–941.

36. Stenjö K., Ow S. Y., Barrios-Llerena M. E., Lindblad P., Wright P. C. 2007. An iTRAQ-based quantitative analysis to elaborate the proteomic response of Nostoc sp. PCC 7120 under N2 fixing conditions. J. Proteome Res. 6:621–635.

37. Sutcliffe I. C. 2010. A phylum level perspective on bacterial cell envelope architecture. Trends Microbiol. 18:464–470.

38. Valladares A., Herrero A., Pils D., Schmetterer G., Flores E. 2003. Cytochrome c oxidase genes required for nitrogenase activity and diazotrophic growth in Anabaena sp. PCC 7120. Mol. Microbiol. 47:1239–1249.

39. Valladares A., Maldener I., Muro-Pastor A. M., Flores E., Herrero A. 2007. Heterocyst development and diazotrophic metabolism in terminal respiratory oxidase mutants of the cyanobacterium Anabaena sp. strain PCC 7120. J. Bacteriol. 189:4425–4430.

40. Valladares A., et al. 2011. Specific role of the cyanobacterial PipX factor in the heterocysts of Anabaena sp. strain PCC 7120. J. Bacteriol. 193:1172–1182.

41. Wilk L., et al. 5 August 2011. Outer membrane continuity and septosome formation between vegetative cells in the filaments of Anabaena sp. PCC 7120. Cell. Microbiol. [Epub ahead of print.] doi:10.1111/j.1462-5822.2011.01655.x.

42. Wolk C. P. 2000. Heterocyst formation in Anabaena, p. 83–104 In Brun Y. B., Shimkets L. J., editors. (ed.), Prokaryotic development. ASM Press, Washington, DC.

43. Wolk C. P., Ernst A., Elhai J. 1994. Heterocyst metabolism and development, p. 769–823 In Bryant D. A., editor. (ed.), The molecular biology of cyanobacteria. Kluwer Academic Publishers, Dordrecht, the Netherlands.

44. Xu X., Elhai J., Wolk C. P. 2008. Transcriptional and developmental responses by Anabaena to deprivation of fixed nitrogen, p. 383–422 In Herrero A., Flores E., editors. (ed.), The cyanobacteria: molecular biology, genomics and evolution. Caister Academic Press, Norfolk, United Kingdom.

Figure captions

Figure 1. Ultrastructure of heterocysts in Anabaena sp. strain PCC 7120 (a and c) and the ΔfraH mutant, strain CSVT4 (b and d). Filaments grown in BG11 medium and incubated for 48 h in BG110 medium (in the absence of combined nitrogen) were prepared for electron microscopy by high-pressure cryo-fixation (a and b) or chemical fixation (c and d) as described in Materials and Methods. Hep, heterocyst envelope polysaccharide; Hgl, heterocyst glycolipid layer; CP, cyanophycin plug; HC, honeycomb intracellular membrane structure. (The cyanophycin plug is frequently lost, leaving a white, empty space in the micrographs, during sample preparation after chemical fixation.) Scale bar, 1 μm.

Figure 2. Ultrastructure of aberrant cells in a ΔfraH mutant. Filaments of strain CSVT4 (ΔfraH) grown in BG11 medium and incubated for 48 h in BG110 medium (in the absence of combined nitrogen) were prepared for electron microscopy by high-pressure cryo-fixation as described in Materials and Methods. A transmission electron micrograph of one sample showing cell doublets (gray arrows) and a dividing cell (white arrow) within a thickened cell envelope is presented; an isolated heterocyst can also be observed (black arrow). CP, cyanophycin plug.

Figure 3. Localization of FraH-C-GFP in the Anabaena filaments. (A) Sequence features of FraH. The region with Cys-X-X-Cys motifs is shown in red, the Pro-rich region is shown in blue, and one possible transmembrane segment is shown in gray (topology according to MEMSAT3 Prediction [http://bioinf.cs.ucl.ac.uk/psipred/]). The position of a putative FHA domain is also indicated. The GFP is not to scale. (B, C, and D) Filaments of Anabaena sp. strain CSVT26 from bubbled cultures grown with nitrate (BG11C; NO_3^-) or incubated in the absence of combined nitrogen for 24 h (BG110C; N_2) were visualized by confocal (B and D) or fluorescence (C) microscopy as described in Materials and Methods. The micrographs show overlays of the cyanobacterial red autofluorescence and the GFP fluorescence. Arrows in panel B point to cells in which the helical pattern of FraH-C-GFP is evident. Arrows in panel D point to an intercalary heterocyst (1), a terminal heterocyst (2), and a proheterocyst presumably released from a broken filament (3). Scale bar, 3 μm.

Figure 4. Localization of FraH-C-GFP during development of heterocyst-containing filaments. Filaments of Anabaena sp. strain CSVT26 grown with nitrate were incubated in the absence of combined nitrogen for 24 h and visualized by confocal microscopy at the indicated times as described in Materials and Methods. Bright field (left), GFP fluorescence (center), and overlays of red cyanobacterial autofluorescence and GFP fluorescence (right) are shown. Identical microscope settings were used for the different time points.

Figure 5. Localization of FraH-C-GFP in heterocysts. Filaments of Anabaena sp. strain CSVT26 grown with nitrate were incubated in the absence of combined nitrogen for 24 h and analyzed by fluorescence microscopy and deconvolution of images. Portions of filaments with a terminal (A) or an intercalary (B) heterocyst are shown. Top, GFP fluorescence; middle, red cyanobacterial autofluorescence and GFP fluorescence overlay; bottom, bright field and GFP fluorescence overlay.

Figure 6. Intercellular transfer of 5-carboxyfluorescein in Anabaena sp. strain PCC 7120 and the ΔfraH mutant. (A) Examples of 5-carboxyfluorescein transfer between vegetative cells in nitrate-grown filaments of strains PCC 7120 (wild type) and CSVT4 (ΔfraH). The arrows indicate the places of bleaching. Fluorescence was then checked at about 2-s intervals showing different degrees of recovery. (B) Recovery rate constant, R, was determined for vegetative cells in nitrate-grown filaments or filaments incubated without combined nitrogen for 24 h

(dinitrogen). Values are the means and standard deviation of the means (n, number of filaments in which FRAP was quantified). Scale bar, 3 μm.

Figure 7. Intercellular transfer of calcein between vegetative cells and heterocysts of Anabaena sp. strain PCC 7120 and the ΔfraH mutant. (A) Examples of calcein transfer between vegetative cells and heterocysts of strains PCC 7120 (wild type) and CSVT4 (ΔfraH). Nitrate-grown filaments incubated for 24 h in the absence of combined nitrogen. The lower panel shows an isolated heterocyst subjected to partial bleaching. The arrows indicate the places of bleaching. (B) Exchange coefficient, E, was determined for calcein transfer from vegetative cells to heterocysts in filaments incubated without combined nitrogen for 24 h or 48 h. Values are the means and standard deviation of the means (n, number of filaments in which FRAP was quantified). Scale bar, 3 μm.

Figure 1

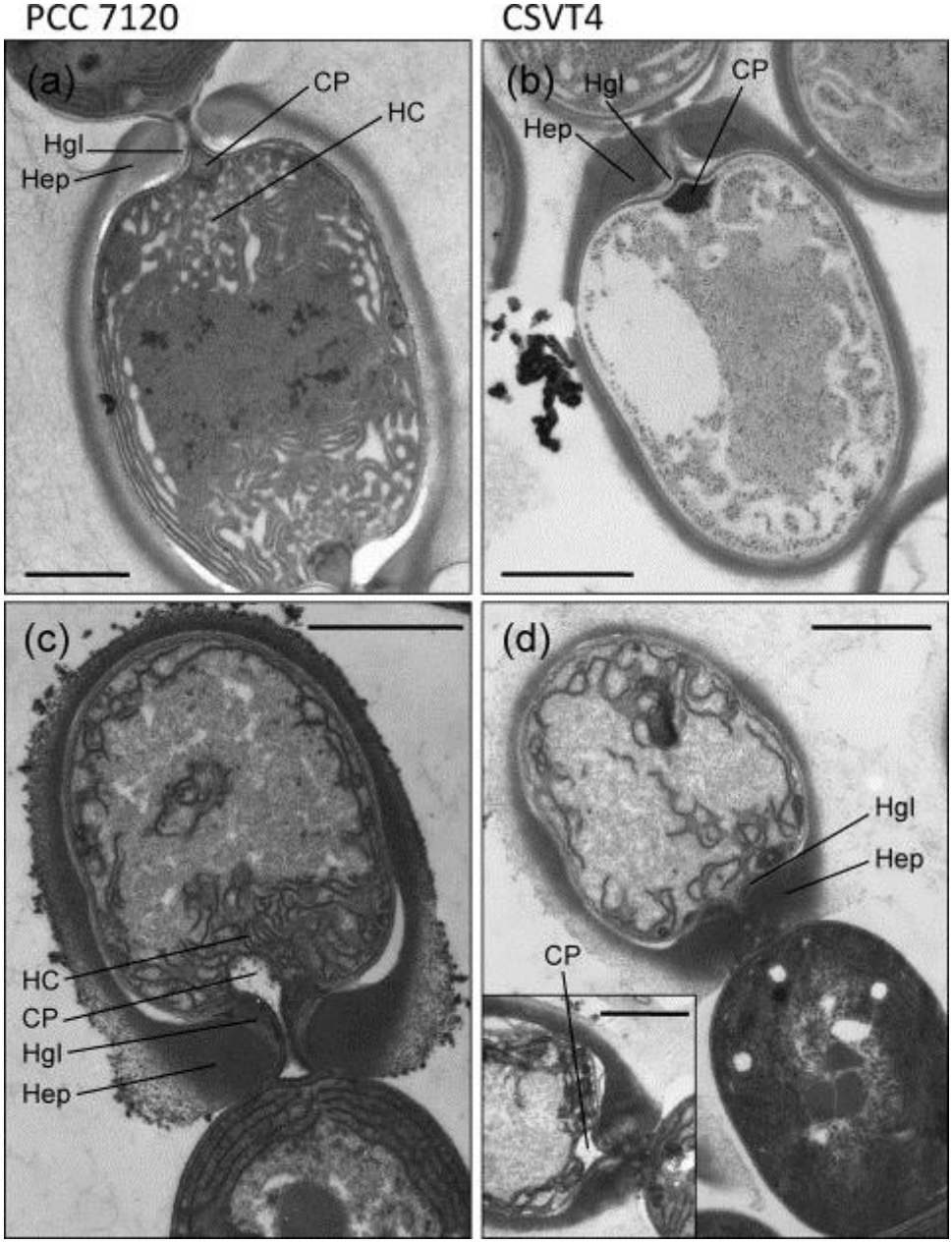
PCC 7120
CSVT4
(a)
CP
HC
Hgl
Hep
(b)
Hgl
CP
Hep
(c)
HC
CP
Hgl
Hep
(d)
Hgl
Hep
CP

Figure 2

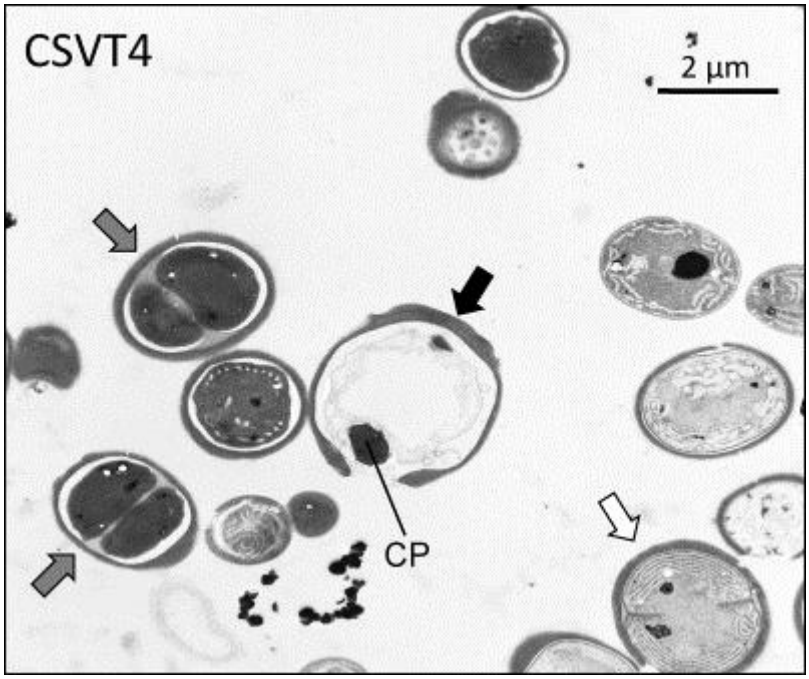

Figure 3

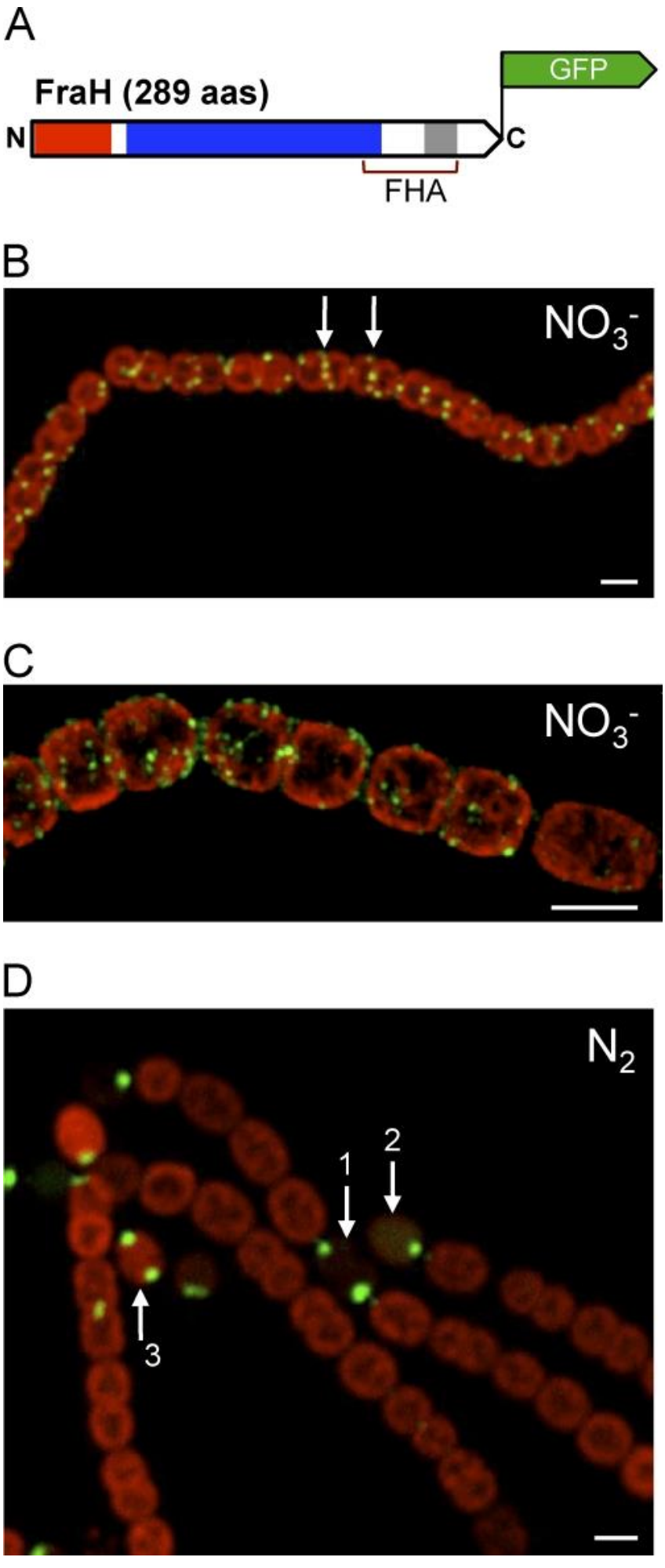

Figure 4

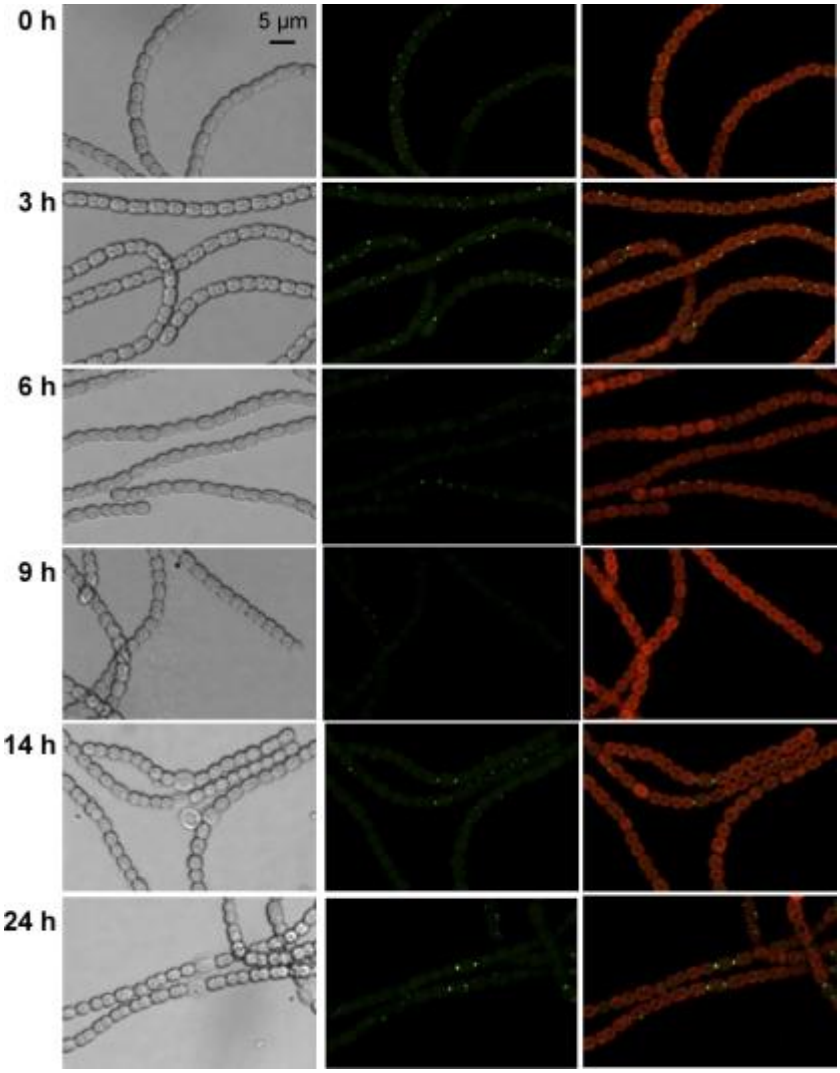

Figure 5

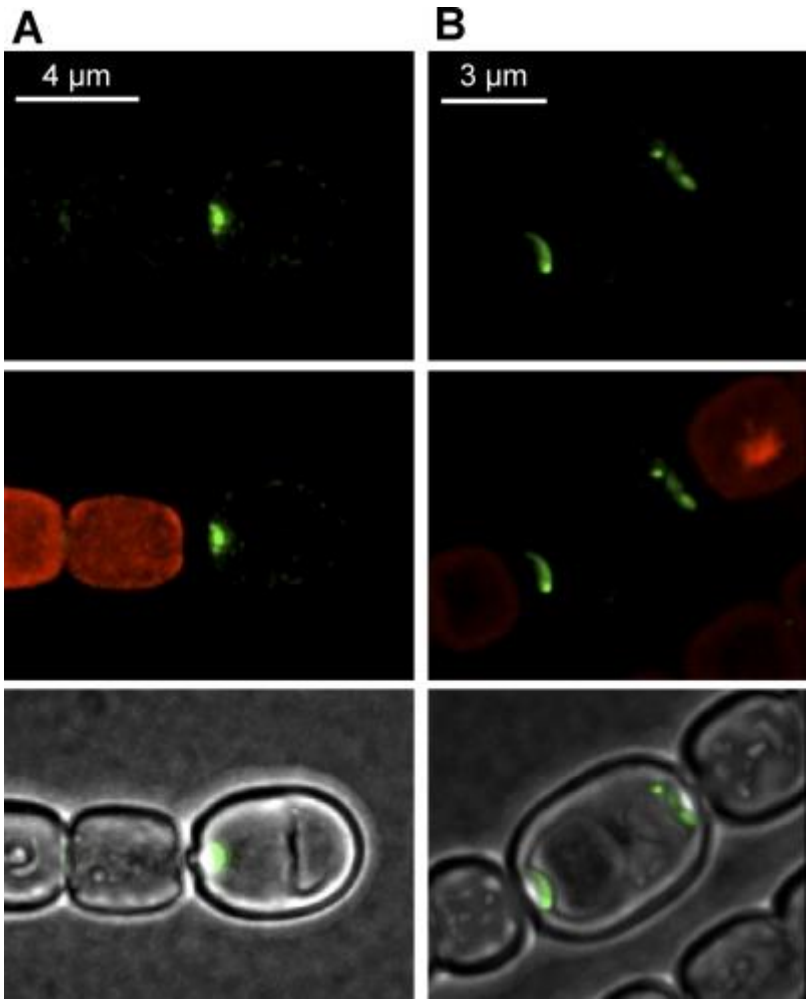

Figure 6

A

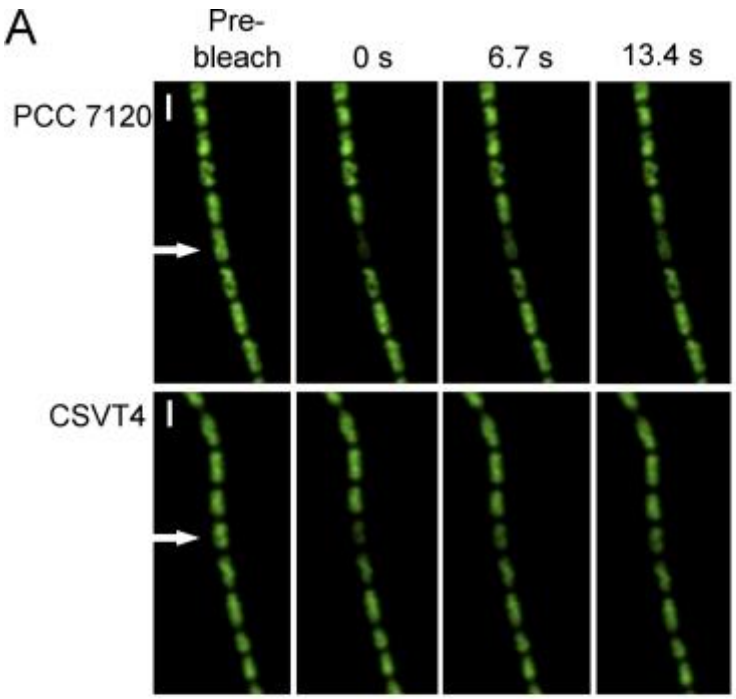

B

Strain	5-CFDA transfer, R (s^{-1})	
	Nitrate	Dinitrogen
PCC 7120 (wt)	0.055 ± 0.002 (*n*=22)	0.059 ± 0.001 (*n*=31)
CSVT4 (Δ*fraH*)	0.054 ± 0.002 (*n*=31)	0.043 ± 0.002 (*n*=32)

Figure 7

A

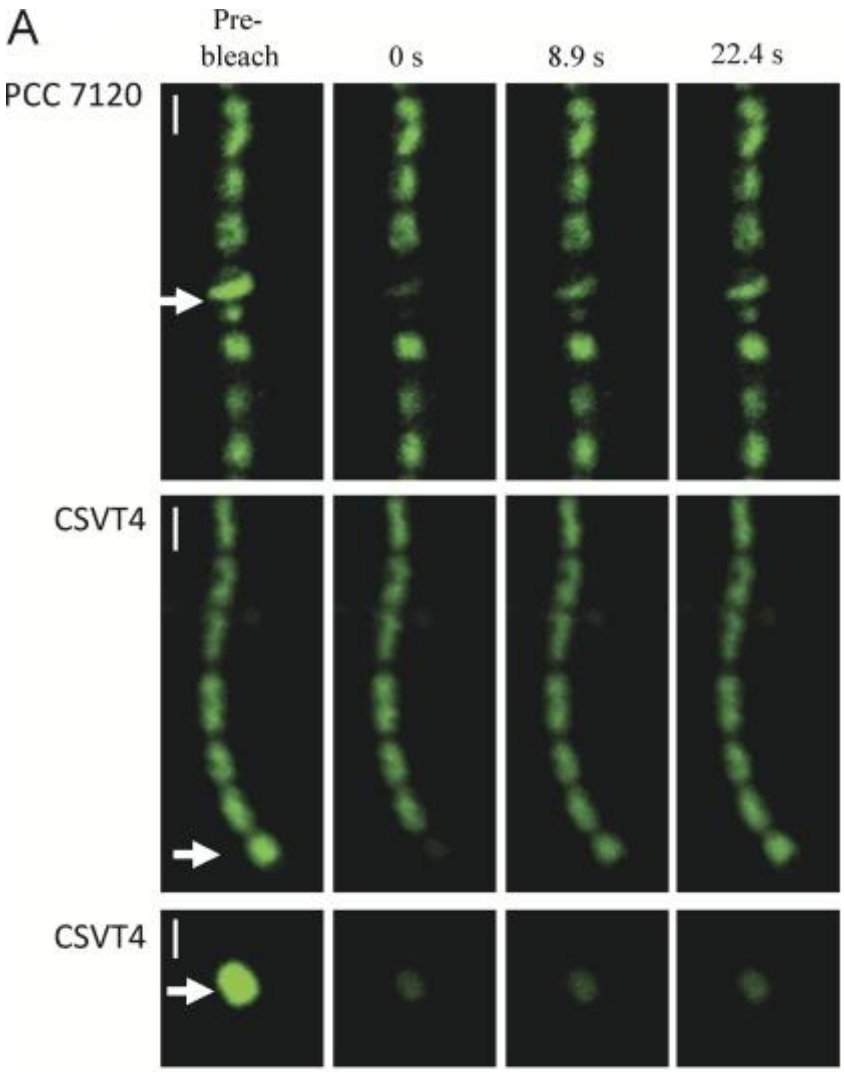

B

Strain	Calcein transfer, E (s^{-1})	
	Dinitrogen (24 h)	Dinitrogen (48 h)
PCC 7120 (wt)	0.033 ± 0.002 (n=7)	0.028 ± 0.001 (n=9)
CSVT4 (Δ*fraH*)	0.074 ± 0.003 (n=9)	0.068 ± 0.005 (n=9)